

## [35] Monitoring Protein Conformations and Interactions by Fluorescence Resonance Energy Transfer between Mutants of Green Fluorescent Protein

By ATSUSHI MIYAWAKI and ROGER Y. TSIEN

### Introduction

#### *Mutants of Green Fluorescent Protein with Altered Colors*

Green fluorescent protein (GFP) is a spontaneously fluorescent protein from the jellyfish *Aequorea victoria*.<sup>1</sup> It can be genetically concatenated to many other proteins, and the resulting fusion proteins are usually fluorescent and often preserve the biochemical functions and cellular localization of the partner proteins. GFP fusions have major advantages over previous techniques for fluorescent labeling of proteins by covalent reaction with small molecule dyes. The chimeric fluorescent proteins are generated *in situ* by gene transfer into cells or organisms, obviating high-level heterologous expression, purification, *in vitro* labeling, and microinjection of recombinant proteins. Targeting signals can be used to direct localization of the chimeras to particular tissues, cells, organelles, or subcellular sites. The sites of labeling are defined exactly, giving a molecularly homogeneous product without the use of elaborate protein chemistry.

Mutagenesis has produced GFP mutants with shifted wavelengths of excitation and emission that can serve as donors and acceptors for fluorescence resonance energy transfer (FRET). FRET is a nondestructive spectroscopic method<sup>2-10</sup> that can be used to monitor the proximity and relative angular orientation of fluorophores in single living cells. The donor and acceptor fluorophores can be on separate proteins to see intermolecular

<sup>1</sup> R. Y. Tsien, *Annu. Rev. Biochem.* **67**, 509 (1998).

<sup>2</sup> L. Stryer, *Annu. Rev. Biochem.* **47**, 819 (1978).

<sup>3</sup> B. Herman, *Methods Cell Biol.* **30**, 219 (1989).

<sup>4</sup> T. M. Jovin and D. J. Arndt-Jovin, *Annu. Rev. Biophys. Biophys. Chem.* **18**, 271 (1989).

<sup>5</sup> P. S. Uster and R. E. Pagano, *J. Cell Biol.* **103**, 1221 (1986).

<sup>6</sup> R. Y. Tsien, B. J. Bacskaï, and S. R. Adams, *Trends Cell Biol.* **3**, 242 (1993).

<sup>7</sup> G. W. Gordon, G. Berry, X. H. Liang, B. Levine, and B. Herman, *Biophys. J.* **74**, 2702 (1998).

<sup>8</sup> P. I. Bastiaens and A. Squire, *Trends Cell Biol.* **9**, 48 (1999).

<sup>9</sup> T. W. J. Gadella, G. N. M. van der Krogt, and T. Bisseling, *Trends Plant Sci.* **4**, 287 (1999).

<sup>10</sup> J. R. Lakowicz, "Principles of Fluorescence Spectroscopy," 2nd Ed. Plenum Press, New York, 1999.

association, or attached to the same macromolecule to detect its conformational changes. Two pairs of GFP mutants have been used for FRET: BFP (blue)–GFP (green) and CFP (cyan)–YFP (yellow).<sup>1,11,12</sup> Further improvements of GFP mutants for FRET have been made as follows. (1) For better folding of GFPs at 37° in mammalian cells, mammalian codon bias and some amino acid substitutions have been introduced to make enhanced fluorescent proteins: EBFP, ECFP, EGFP, and EYFP<sup>1,13</sup>; (2) (E)YFP (S65G/S72A/T203Y) proved to be highly sensitive around neutral pH ( $pK_a$  7). Two amino acid substitutions (V68L/Q69K) were found to lower its  $pK_a$  to about 6.<sup>14</sup> EYFP-V68L/Q69K or EYFP.1 (S65G/V68L/Q69K/S72A/T203Y) is less pH sensitive and therefore a more reliable acceptor than the original EYFP for most applications. In the remainder of this chapter we use the terms CFP and YFP to mean the generic classes of cyan and yellow mutants, whereas EYFP and EYFP.1 refer to the specific variants listed above.

### *Monitoring Fluorescence Resonance Energy Transfer via Emission Ratioing*

Steady state FRET is most conveniently observed by exciting the sample at the donor excitation wavelengths while measuring the ratio of fluorescence intensities emitted at wavelengths corresponding to the emission peaks of the donor (donor channel) versus those of the acceptor (FRET channel). The occurrence of FRET diminishes the signal in the donor channel while increasing the amplitude of the FRET channel. However, simple measurements of the intensities in the two channels and their ratio are perturbed by several factors other than the FRET efficiency. These interfering factors include uncertainties in the relative concentrations of donor and acceptor and spectral cross-talk of two main kinds: (1) direct excitation of the acceptor at the donor excitation wavelengths, and (2) leakage of donor emission into the FRET channel. Leakage of acceptor fluorescence into the donor channel is hardly ever a problem because emission spectra usually cut off quite abruptly at their short-wavelength borders.

These uncertainties are minimized if both the donor and acceptor are

<sup>11</sup> R. Y. Tsien and D. C. Prasher, "GFP: Green Fluorescent Protein Strategies and Applications" (M. Chalfie and S. Kain, eds.). John Wiley & Sons, New York, 1998.

<sup>12</sup> R. Heim, *Methods Enzymol.* **302**, 408 (1999).

<sup>13</sup> A. Miyawaki, J. Llopis, R. Heim, J. M. McCaffery, J. A. Adams, M. Ikura, and R. Y. Tsien, *Nature (London)* **388**, 882 (1997).

<sup>14</sup> A. Miyawaki, O. Griesbeck, R. Heim, and R. Y. Tsien, *Proc. Natl. Acad. Sci. U.S.A.* **96**, 2135 (1999).

fused to the same partner protein to form a three (or more)-component chimera whose conformation is sensitive to the biochemical environment. Obviously the stoichiometry of donor and acceptor is then fixed. Although spectral cross-talk reduces the dynamic range over which the emission ratio can vary, that emission ratio for any given construct can still be empirically calibrated in terms of the extent of biochemical reaction. The first examples of such chimeras were simple fusions of BFPs and GFPs to protease-sensitive linkers. Proteolysis of such linkers *in vitro* disrupted FRET.<sup>15,16</sup> More recently, fusions with linkers cleavable by important intracellular proteases have been introduced to assay the activity of those proteases in living cells.<sup>17</sup> However, these assays still monitor irreversible hydrolysis of covalent bonds. Could the same principle of FRET between different colors of GFP be used to monitor reversible conformational equilibria and fluctuating intracellular signals? Our first successful demonstration of the feasibility of this principle was a family of  $\text{Ca}^{2+}$  indicators, as explained below.

## Construction of Cameleons, Indicators for $\text{Ca}^{2+}$ Based on Calmodulin

### *Initial Design and Screening*

Many effects of  $\text{Ca}^{2+}$  in cells are mediated by the binding of  $\text{Ca}^{2+}$  to calmodulin, which causes calmodulin to bind and activate target proteins. Ikura and collaborators solved the nuclear magnetic resonance solution structure of calmodulin bound to M13,<sup>18</sup> the 26-residue calmodulin-binding peptide of myosin light-chain kinase. They then fused the C terminus of calmodulin to M13 by means of a Gly-Gly spacer and verified that this hybrid protein changed from a dumbbell-like extended form to a compact globular structure on binding  $\text{Ca}^{2+}$ . This hybrid protein, calmodulin-M13, gave us a potential starting point for a  $\text{Ca}^{2+}$  indicator. We initially sandwiched calmodulin-M13 between BFP and S65T.<sup>13</sup> The chimeric proteins (see Fig. 1 for generic structure) were expressed in bacteria and analyzed for FRET. The amino acid sequences of the boundary regions between the calmodulin-M13 hybrid and the GFPs proved critical to the optimization of protein folding (formation of chromophore) and  $\text{Ca}^{2+}$ -dependent changes in FRET. Numerous deletions, insertions, and amino acid substitutions were tested, as shown in Table I.

<sup>15</sup> R. Heim and R. Y. Tsien, *Curr. Biol.* **6**, 178 (1996).

<sup>16</sup> R. D. Mitra, C. M. Silva, and D. C. Youvan, *Gene* **173**, 13 (1996).

<sup>17</sup> X. Xu, A. L. V. Gerard, B. C. B. Huang, D. C. Anderson, D. G. Payan, and Y. Luo, *Nucleic Acids Res.* **26**, 2034 (1998).

<sup>18</sup> M. Ikura, G. M. Clore, A. M. Gronenborn, G. Zhu, C. B. Klee, and A. Bax, *Science* **256**, 632 (1992).

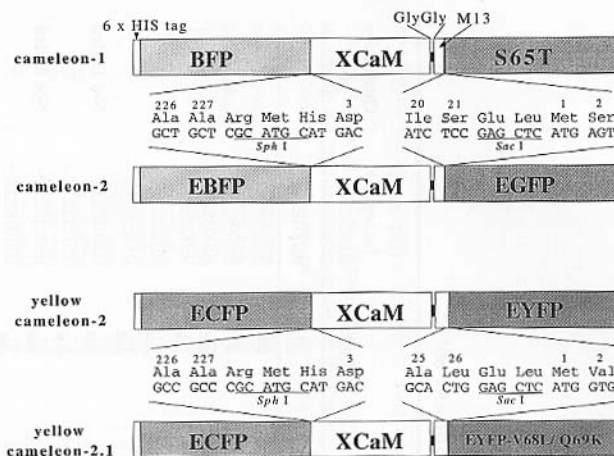


FIG. 1. Domain structures of cameleons (cameleon-1, cameleon-2, YC2, and YC2.1) expressed in bacteria for *in vitro* characterization, showing sequences of the boundaries between the donor GFP and *Xenopus* calmodulin (XCaM) and between M13 and the acceptor GFP.

**Folding and Fluorescence of Green Fluorescent Protein Mutants.** Intramolecular FRET obviously requires that both the donor and acceptor GFPs remain fluorescent after fusion. However, in many variants of our chimeras, either the BFP or the S65T was not fluorescent, probably because of misfolding. Also, some of the chimeras were easily proteolyzed in bacteria or during purification. Resistance to proteolysis of the chimeras was finally checked in mammalian cells; in HeLa cells transfected with the cDNAs, the intact chimera was uniformly distributed in the cytosolic compartment but excluded from the nucleus, as expected for a 74-kDa protein without targeting signals. On the other hand, the chimeras that were susceptible to proteolysis entered the nucleus. Although we earlier referred to the molecular homogeneity of GFP-fused proteins, trial and error is often necessary to obtain fusions that express well without precipitation or proteolysis.

**Responsivity of Fluorescence to  $Ca^{2+}$ .** Only intact chimeras containing both functional BFP and S65T were screened for responsivity to  $Ca^{2+}$ . Sometimes only one amino acid substitution changed the FRET efficiency dramatically; we found it impossible to predict in advance what sorts of amino acid sequences should be put in the boundaries (Table I). Empirically, we found it better to fuse the two GFPs rigidly to the calmodulin-M13 hybrid protein without extra spacers at the boundaries, leaving the Gly-Gly spacer between the calmodulin and M13 as the only obvious hinge in the whole chimera. Thus removal of the 11 C-terminal amino acids of the BFP, slightly more than the 9 residues too disordered to be seen in the

TABLE I  
VARIOUS CHIMERIC PROTEINS FOR  $\text{Ca}^{2+}$  INDICATORS CONTAINING BFP AND S65T<sup>a</sup>

Chimera	BFP (donor) (-AAGITHGMDLYK)	<i>Xenopus</i> calmodulin (MHDQLTEEQIAEFKE---TAK)	Linker	M13 peptide (RRW---FKKISSSGAL)	Linker	GFP:S65T (acceptor) (MSKGEELF-)	Qualitative grade
1	-AAGITHMDELYK	GAGMHDQLTEEQIAEFKE---TAK	GGK	RRW---FKKISSSGAL	EL	MSKGEELF-	C <sup>b</sup>
2	-AGIATHG	MHDQLTEEQIAEFKE---TAK	GGK	RRW---FKKISSSGAL	EL	MSKGEELF-	B
3	-AAGITHG	MREEQIAEFKE---TAK	GGK	RRW---FKKISSSGAL	EL	MSKGEELF-	B
4	-AAGITHG	MQEEQIAEFKE---TAK	GGK	RRW---FKKISSSGAL	EL	MSKGEELF-	C
5	-AAGITHG	MHEEQIAEFKE---TAK	GGK	RRW---FKKISSSGAL	EL	MSKGEELF-	C
6	-AAGITHG	MLEEQIAEFKE---TAK	GGK	RRW---FKKISSSGAL	EL	MSKGEELF-	C
7	-AAGITHG	MPREEQIAEFKE---TAK	GGK	RRW---FKKISSSGAL	EL	MSKGEELF-	C
8	-AAGITHG	MLOIAEFKE---TAK	GGK	RRW---FKKISSSGAL	EL	MSKGEELF-	Not folded
9	-AGIT#	MHDQLTEEQIAEFKE---TAK	GGK	RRW---FKKISSSGAL	EL	MSKGEELF-	D
10	-AAC	MHDQLTEEQIAEFKE---TAK	GGK	RRW---FKKISSSGAL	EL	MSKGEELF-	Not folded
11	-AAR	MHDQLTEEQIAEFKE---TAK	GGK	RRW---FKKISSSGAL	EL	MSKGEELF-	B
12	-AAG	MHDQLTEEQIAEFKE---TAK	GGK	RRW---FKKISSSGAL	EL	MSKGEELF-	C
13	-AAS	MHDQLTEEQIAEFKE---TAK	GGK	RRW---FKKISSSGAL	EL	MSKGEELF-	C
14	-AAR	MHDQLTEEQIAEFKE---TAK	GGK	RRW---FKKISSSG	EL	MSKGEELF-	B
15	-AAR	MHDQLTEEQIAEFKE---TAK	GGK	RRW---FKKIS	EL	MSKGEELF-	A

16	-AAR	MH QLTEEQIAEFKE---TAK	GGK	RRW---FKKIS	EL	MSKGEELF-	D
17	-AAR	M QLTEEQIAEFKE---TAK	GGK	RRW---FKKIS	EL	MSKGEELF-	Not folded
18	-AAR	MHDQLTEEQIAEFKE---TAK	GGK	RRW---FKKIA	EL	MSKGEELF-	B
19	-AAR	MHDQLTEEQIAEFKE---TAK	GGK	RRW---FKKIC	EL	MSKGEELF-	B
20	-AAR	MHDQLTEEQIAEFKE---TAK	GGK	RRW---FKKI	EL	MSKGEELF-	B
21	-AAR	M #EEQIAEFKE---TAK	GGK	RRW---FKKISSGAL	EL	MSKGEELF-	C
22	-AAR	M #EQIAEFKE---TAK	GGK	RRW---FKKISSGAL	EL	MSKGEELF-	B
23	-AAR	M LQIAEFKE---TAK	GGK	RRW---FKKISSGAL	EL	MSKGEELF-	C
24	-AAR	M QIAEFKE---TAK	GGK	RRW---FKKISSGAL	EL	MSKGEELF-	A
25	-AAR	M #EEQIAEFKE---TAK	GGK	RRW---FKKIS	EL	MSKGEELF-	Not folded
26	-AAR	M LQIAEFKE---TAK	GGK	RRW---FKKIS	EL	MSKGEELF-	Not folded
27	-AAR	MHDQLTEEQIAEFKE---TAK	GGGS	RRW---FKKIS	EL	MSKGEELF-	Proteolyzed
28	-AAR	MHDQLTEEQIAEFKE---TAK	(GGS) 4	RRW---FKKIS	EL	MSKGEELF-	Proteolyzed

<sup>a</sup> The genes for BFP and *Xenopus* calmodulin were linked using an *Sph*I site; the amino acid sequences encoded by the *Sph*I site are underlined. The underlined amino acid sequences (EL) between the M13 peptide and S65T are encoded by an *Sac*I site. #, Introduced amino acid has not been determined. The quality of the Ca<sup>2+</sup>-dependent change in FRET was qualitatively graded as A-D, with A being the best. Chimera 15 gave above 80% change in FRET, and was termed cameleon-1.

<sup>b</sup> The change in FRET was not reversible. "Not folded" indicates either the BFP or the S65T was not fluorescent, or the whole protein was not synthesized. "Proteolyzed" indicates proteolysis occurred between calmodulin and M13 peptide.

BFP or GFP crystal structures,<sup>19,20</sup> improved the  $\text{Ca}^{2+}$ -dependent change in FRET significantly. The capriciousness of these permutations made us call these  $\text{Ca}^{2+}$  indicators "cameleons." Like real chameleons, they readily change color, and retract and extend a long tongue (M13) into and out of the mouth of the calmodulin (CaM).

We tried to select bacterial clones producing good  $\text{Ca}^{2+}$  indicator proteins by measuring FRET directly from colonies on a plate, when they were soaked with  $\text{Ca}^{2+}$  and then EGTA in the presence of  $\text{Ca}^{2+}$  ionophore. But the signals obtained depended on many factors other than  $\text{Ca}^{2+}$ : size of colony, degree of misfolding and/or proteolysis inside bacteria, efficiency of exposure of the proteins to the reagents, and so on. Because quantitation of FRET in colonies was unreliable, we had to purify each protein, check its integrity, and then analyze FRET. An alternative screening system would be fluorescence-activated cell sorting (FACS), which measures fluorescence from every bacterium. Unfortunately, FACS is not suited to comparing the fluorescence of given clones before and after a manipulation such as changing the  $\text{Ca}^{2+}$ .

The efficiency of FRET theoretically should not be affected by exchanging the positions of the donor and acceptor fluorophores, because the distance between the chromophores and the orientation factor remains unchanged. However, the quality of chimeric proteins is not necessarily the same in the two cases. In our experience, when two GFPs are fused to the N and C termini of a host protein, the N-terminal GFP is generally better folded than the C-terminal GFP. In our initial screens we put the BFP at the N terminus and S65T at the C terminus, because the fluorescence of the latter is more reliably seen by eye and would imply that both GFPs must have folded correctly. In such complete constructs, we tried exchanging the BFP and S65T, but these chimeras (S65T-calmodulin-M13-BFP) empirically showed a somewhat smaller  $\text{Ca}^{2+}$ -dependent FRET response, about 1.65-fold maximal ratio change, compared with 1.8 to 1.9-fold for BFP-CaM-M13-S65T. Therefore we settled on the latter ordering.

*Importance of Relative Orientations of Green Fluorescent Protein Mutants.* Multidimensional nuclear magnetic resonance (NMR) had shown that the  $\text{Ca}^{2+}$ -saturated calmodulin-M13 hybrid protein shows a compact globular structure similar to that of the  $\text{Ca}^{2+}$ -calmodulin-M13 intermolecular complex.<sup>18</sup> The three-dimensional structure of the  $\text{Ca}^{2+}$ -free, extended

<sup>19</sup> R. M. Wachter, B. A. King, R. Heim, K. Kallio, R. Y. Tsien, S. G. Boxer, and S. J. Remington, *Biochemistry* **36**, 9759 (1997).

<sup>20</sup> M. Ormö, A. B. Cubitt, K. Kallio, L. A. Gross, R. Y. Tsien, and S. J. Remington, *Science* **273**, 1392 (1996).

form of the hybrid protein has not been solved, although Porumb *et al.*<sup>21</sup> showed that its conformation differed from that of the  $\text{Ca}^{2+}$  complex. Furthermore, we do not know how the two GFPs fused to the hybrid protein are positioned. Current indications are that the  $\text{Ca}^{2+}$ -dependent increase in FRET is due more to a change in the relative orientations of the two GFP chromophores rather than the distance between them. The belief is based on observations that small structural alterations such as adding or subtracting single amino acids from the linker regions, or substituting a circularly permuted CFP for native CFP,<sup>22</sup> can cause profound changes in the effect of  $\text{Ca}^{2+}$  on FRET. Such alterations should not greatly affect the distance between the chromophores but could well change their relative orientations drastically.

### *Expression of Cameleon in Mammalian Cells*

The prototype cameleon, cameleon-1 (Fig. 1), was efficiently expressed and folded in bacteria and increased its ratio of ultraviolet-excited 510:445 nm emissions by 70% on binding  $\text{Ca}^{2+}$ . The decrease in blue and increase in green emission indicated that  $\text{Ca}^{2+}$  increased the efficiency of FRET from BFP to S65T, consistent with the expected decrease in distance between the two ends of the protein. Cameleon-1 displayed a biphasic  $\text{Ca}^{2+}$  dependency with apparent dissociation constants of 70 nM and 11  $\mu\text{M}$ , and therefore could report a wide range of  $\text{Ca}^{2+}$  concentration from  $10^{-9}$  to  $10^{-4}$  M. Despite the promising  $\text{Ca}^{2+}$  sensitivity observed in *in vitro* experiments, the fluorescence of cameleon-1 was not bright enough for  $\text{Ca}^{2+}$  imaging in mammalian cells. For adequate expression and brightness of the mutant GFPs in mammalian cells, enhanced GFPs (EBFP and EGFP) encoded by sequences containing mammalian codon usage and including amino acid mutations for improved folding at 37° were developed.<sup>1</sup> The substitution of EBFP and EGFP for BFP and S65T improved the expression of cameleon in mammalian cells. The resulting cameleon, cameleon-2 (Fig. 1), was able to report agonist-evoked changes in cytosolic  $\text{Ca}^{2+}$  concentration ( $[\text{Ca}^{2+}]_c$ ) in HeLa cells. Cameleon-2 also appeared to be expressed better than cameleon-1 in bacteria.

### *Longer-Wavelength Cameleons*

Another concern was that blue mutants such as EBFP are the dimmest and most bleachable of the GFPs. Their excitation peaks are in the ultraviolet-

<sup>21</sup> T. Porumb, P. Yau, T. S. Harvey, and M. Ikura, *Protein Eng.* **7**, 109 (1994).

<sup>22</sup> G. S. Baird, D. A. Zacharias, and R. Y. Tsien, *Proc. Natl. Acad. Sci. U.S.A.* **96**, 11241 (1999).



let at 382 nm, which is potentially injurious, excites the most cellular autofluorescence, and could interfere with the use of caged compounds. Therefore, enhanced cyan and yellow fluorescent proteins (ECFP and EYFP) were substituted for EBFP and EGFP, respectively, to make "yellow cameleons" (YCs). ECFP has two excitation peaks of nearly equal amplitude at 434 and 452 nm. To minimize direct excitation of the acceptor, the ECFP should be excited at the 434-nm peak or even shorter wavelengths, and the acceptor should be EYFP rather than EGFP. Another theoretical advantage of the ECFP–EYFP pair is that it gives stronger FRET than EBFP–EGFP, assuming other factors are equal. The calculated distance  $R_0$  at which FRET is 50% efficient between randomly oriented chromophores is 5 nm for ECFP–EYFP versus 4 nm for EBFP–EGFP.<sup>12</sup> Accordingly, the boundary regions were reoptimized for maximal  $\text{Ca}^{2+}$  dependence of FRET; the C terminus of the M13 peptide in YCs was extended by five amino acids. The resulting YCs showed 1.8- to 1.9-fold changes in emission ratio from zero to saturating  $\text{Ca}^{2+}$ .

#### *pH Sensitivity of Green Fluorescent Protein Based Fluorescence Resonance Energy Transfer*

Intracellular pH varies among organelles and under conditions such as mitogen stimulation and metabolic stress. If FRET is used to measure protein conformations or interactions in intact cells, the donor and acceptor should be indifferent to physiological changes in pH. However, every GFP mutant is at least somewhat pH sensitive, in that all can be quenched by sufficiently acidic pH. The most important effects of pH are on the quantum efficiency of the donors EBFP and ECFP (Fig. 2) and the absorbance spectra of the acceptors EGFP and EYFP (Fig. 3). Decreasing pH quenches the emissions of EBFP and ECFP with little effect on their absorbance spectra, indicating that their quantum yields are depressed by acid, but the effects are not serious until the pH falls below 6. However, the original EYFP has quite a high  $\text{pK}_a$  of 6.9 for both its absorbance and emission spectra<sup>23</sup> (Fig. 3), indicating that its absorbance, not its quantum yield, is pH sensitive. This  $\text{pK}_a$  is uncomfortably close to cytosolic pH, rendering the first generation of cameleons quite pH sensitive. The obvious solution was to find a less pH-sensitive version of EYFP. Adding the mutation Q69K to 10C (S65G, V68L, S72A, T203Y) dropped the apparent  $\text{pK}_a$  to 6.1,<sup>14</sup> decreasing the sensitivity to pH changes between 6 and 8 (Fig. 3). 10C Q69K (EYFP-V68L/Q69K or EYFP.1) could be substituted for the original EYFP without altering the  $\text{Ca}^{2+}$ -dependent FRET changes of YCs, because

<sup>23</sup> J. Llopis, J. M. McCaffery, A. Miyawaki, M. G. Farquhar, and R. Y. Tsien, *Proc. Natl. Acad. Sci. U.S.A.* **95**, 6803 (1998).

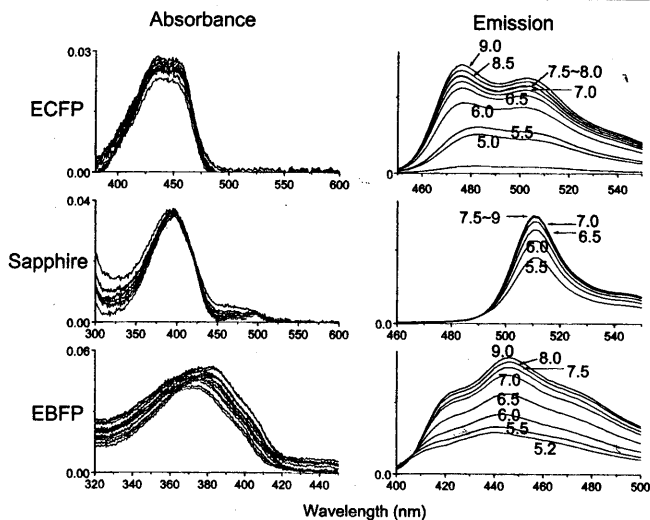


FIG. 2. pH dependency of donor GFPs. *Left*: Absorbance spectra of EBFP (F64L/Y66H/Y145F), Sapphire (T203I/S72A/Y145F), and ECFP (F64L/S65T/Y66W/N146I/M153T/V163A/N164H) in buffers of different pH. The individual spectra are not labeled because they are so nearly overlapping. "Sapphire" (synonymous with "H9-40") is a UV-excited, green-emitting mutant<sup>1,12</sup> included here for completeness, although it is of little utility as an FRET donor to EGFP or EYFP because its emission overlaps too greatly with theirs. *Right*: Emission spectra measured in buffers of the indicated pH. Excitation was at 380 nm for EBFP, 400 nm for Sapphire, and 432 nm for ECFP.

the two EYFPs have the same fluorescence properties other than pH sensitivity. YC2 incorporating EYFP.1 was constructed and termed YC2.1 (Fig. 1). The best samples of YC2.1 now show emission ratio changes of 2.0- to 2.1-fold between zero and saturating  $\text{Ca}^{2+}$ ; the slight improvement over YC2 is probably due to better protein purification rather than to the V68L/Q69K mutations.

Despite the improvement in  $pK_a$  values, pH sensitivity should not be forgotten. Checking or clamping of ambient pH is still desirable to prevent artifacts. It is unfortunate that acidity causes the donors to lose quantum yield and the acceptors to lose absorbance, because the two negative effects reinforce each other. Had the losses been in donor absorbance or acceptor quantum yield, they would not have affected the efficiency of FRET.

#### *Future Prospects for Improvement of Cameleons*

Aside from their pH sensitivity, the YFPs have other drawbacks as FRET acceptors, such as their small Stokes shift and their photochemical

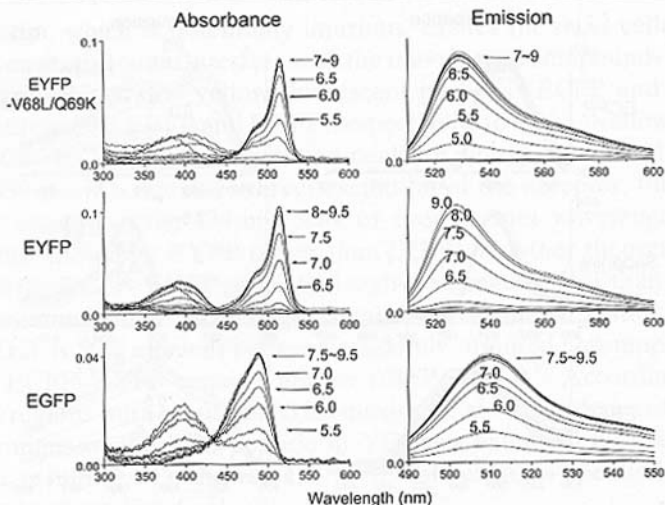


FIG. 3. pH dependency of acceptor GFPs. *Left*: Absorbance spectra of EYFP.1 (S65G/V68L/Q69K/S72A/T203Y), EYFP (S65G/S72A/T203Y), and EGFP (F64L/S65T) at the indicated pH. *Right*: pH dependency of emission spectra of the acceptor GFPs. Excitation was at 500 nm for EYFP.1 and EYFP, and at 480 nm for EGFP.

instability (photochromism) at high light intensities,<sup>24</sup> although as will be seen, the photochromism can be useful for quantifying FRET. More recently, novel yellow and red fluorescent proteins have been cloned from corals.<sup>25</sup> Although these new proteins have not yet been fully characterized or optimized for mammalian expression, they offer the exciting prospect of accepting FRET from EGFP. Such pairs would use a donor whose quantum yield is pH independent and allow us to make "red cameleons."

Advances in single-molecule detection and single-molecule spectroscopy by laser-induced fluorescence offer new tools for the study of individual macromolecules.<sup>13</sup> It has become possible to observe the fluorescence from single molecules of YC2.1, trapped in agarose gels to prevent lateral diffusion.<sup>25a</sup>

### Procedures

Here we present a series of *in vitro* experiments for YC2.1.

<sup>24</sup> R. M. Dickson, A. B. Cubitt, R. Y. Tsien, and W. E. Moerner, *Nature (London)* **388**, 355 (1997).

<sup>25</sup> M. V. Matz, A. F. Fradkov, Y. A. Labas, A. P. Savitsky, A. G. Zaraisky, M. L. Markelov, and S. A. Lukyanov, *Nature Biotechnol.* **17**, 969 (1999).

<sup>25a</sup> S. Brasselet, A. Miyawaki, and W. E. Moerner, Submitted (2000).

**Expression and Purification of Recombinant YC2.1 Protein.** The YC2.1 coding sequence is subcloned into *Bam*HI and *Eco*RI restriction sites of expression plasmid pRSETB (InVitrogen, San Diego, CA), which encodes a fusion protein containing a six-histidine ( $\text{His}_6$ ) tag and an enterokinase cleavage site upstream from the insert. For bacterial expression, *Escherichia coli* JM109(DE3) is transformed with the plasmid and grown on LB plates containing ampicillin (0.1 mg/ml). A 2-ml overnight culture is used to inoculate 100–500 ml of medium. Overgrowth of the colonies and cultures before inoculation should be avoided. The bacteria are grown at 25° to an optical density of 0.4–0.8 at 600 nm and induced with 0.1–1 mM isopropyl-thiogalactoside for 12–24 hr. Cells are harvested by centrifugation. The bacterial pellet looks greenish-yellow, primarily due to the absorption of ECFP and EYFP.1. The pellet is resuspended in 30 ml of phosphate-buffered saline (PBS), pH 7.4, and lysed with a French press in the presence of protease inhibitors (leupeptin, pepstatin A, and phenylmethylsulfonyl fluoride). The lysate is then clarified by centrifuging at 12,000g for 30 min at 4°. Efficient extraction by a French press gives a greenish-yellow supernatant and a whitish pellet of cellular debris. Binding of the  $\text{His}_6$  tag to Ni-NTA agarose (Qiagen, Chatsworth, CA) is carried out in a batch mode; the supernatant is transferred to a new tube, to which 0.5–1 ml of the 50% (v/v) Ni-NTA slurry is added, and mixed gently on a rotary shaker at 4° for 1 hr. The lysate–Ni-NTA mixture is loaded into a column, which is washed with 10 volumes of PBS, and then with 10 volumes of TN300 buffer [Tris-HCl (pH 7.4), 300 mM NaCl]. The recombinant YC2.1 protein is eluted with 1–3 ml of elution buffer (100 mM imidazole in TN300). Imidazole is removed by passing the eluate through a Sephadex G-25 column, eluting with buffer A [50 mM HEPES–KOH (pH 7.4), 100 mM NaCl]. The protein sample is concentrated with a Centricon 30 filter (Amicon, Danvers, MA), and then used for size-exclusion or ion-exchange chromatography.

**Monitoring the Integrity of YC2.1.** Figure 4 shows elution profiles of the concentrated eluates obtained by size-exclusion chromatography. A size-exclusion column (Biosep SEC-S3000, 300 × 7.5 mm; Phenomenex, Torrance, CA) is equilibrated with buffer A, and is linked to absorbance (at 280 nm) and fluorescence (excitation at 432 nm; emission at 502 or 528 nm) detectors. Thus the effluent is monitored on line for total protein concentration and for concentration of the desired protein at the same time. YC2.1 recombinant protein is eluted in almost a single peak (Fig. 4A). A slight shoulder on the right side may represent minor proteolysis. These results indicate that nearly all the proteins in the Ni-NTA eluate are full-length YC2.1. In contrast, Fig. 4B shows a chimera containing the linker GGSGGSGGS instead of the GG used in YC2.1. This protein sample is

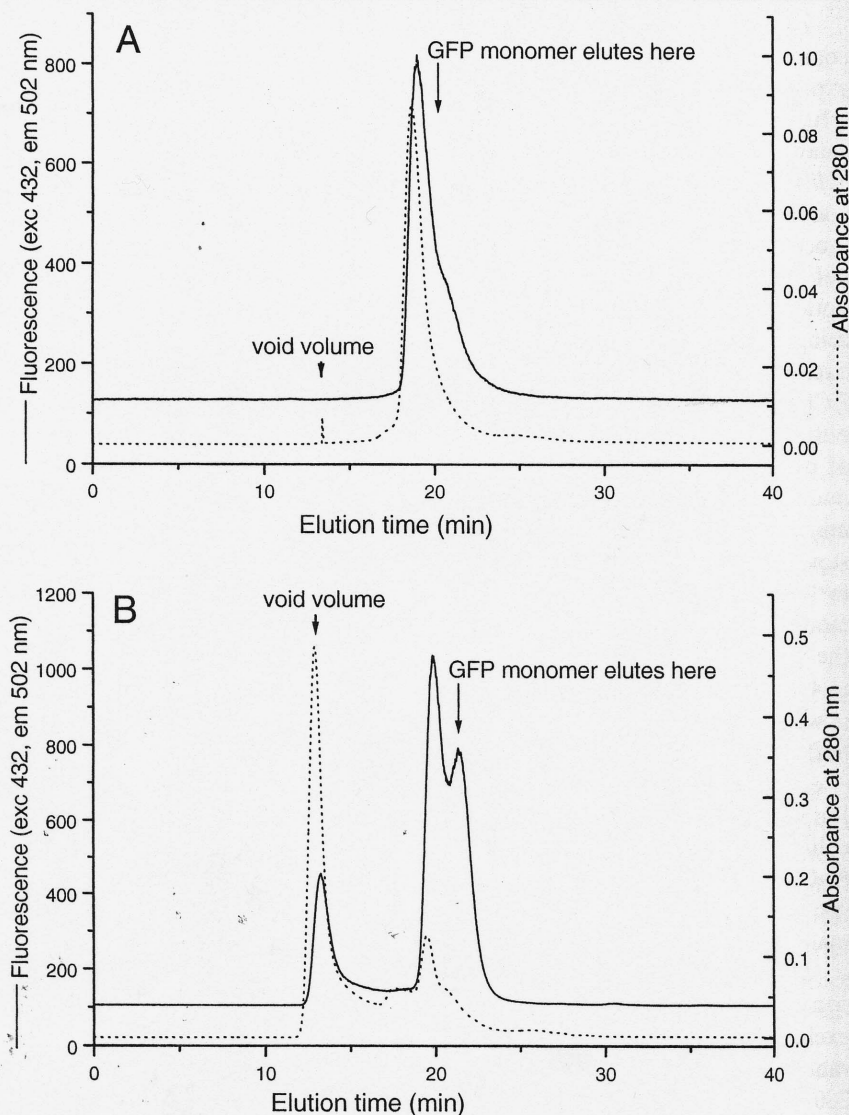


FIG. 4. Size-exclusion chromatography of fluorescent proteins. Total protein and the fluorescence of ECFP were monitored by absorbance at 280 nm (dashed lines) and by fluorescence (solid lines; excitation at 432 nm, emission at 502 nm). The void volume and the elution position for GFP monomer are indicated. The absorbance peaks appear slightly earlier than the matching fluorescence peaks because the effluent passed first through the absorbance detector, and then through the fluorescence detector. (A) Elution profiles for recombinant YC2.1 protein purified by Ni-NTA chromatography. (B) Elution profiles for an unsatisfactory chimera with GGSGGSGGS instead of GG as the linker between the CaM and M13.

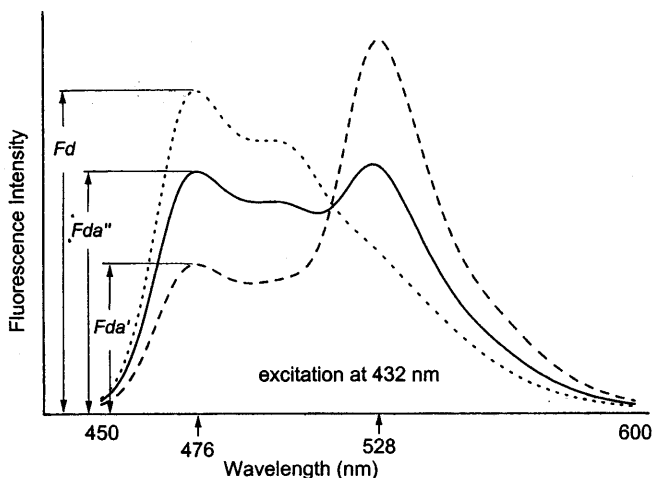


FIG. 6. Emission spectra of YC2.1 (excited at 432 nm) of the  $\text{Ca}^{2+}$ -saturated (dashed line) and  $\text{Ca}^{2+}$ -unsaturated (solid line) forms, and after proteolysis by trypsin (dotted line). The wavelengths giving the emission peaks of ECFP (476 nm) and EYFP.1 (528 nm) are indicated.

quantitate the FRET of the  $\text{Ca}^{2+}$ -saturated and  $\text{Ca}^{2+}$ -unsaturated forms, by measuring the fluorescence intensity of donor both in the absence ( $F_d$ ) and presence ( $F_{da}$ ) of acceptor. Generally, the efficiency of FRET ( $E$ ) is given by Eq. (1)<sup>10</sup>:

$$E = 1 - (F_{da}/F_d) \quad (1)$$

At a wavelength of 476 nm, ECFP (donor) exhibits a major emission peak, whereas EYFP.1 (acceptor) does not emit light at all; the fluorescence emission at 476 nm comes only from the donor (Fig. 5). Therefore  $F'_{da}$  and  $F''_{da}$  in Fig. 6 are the  $F_{da}$  values of the  $\text{Ca}^{2+}$ -saturated and  $\text{Ca}^{2+}$ -unsaturated forms, respectively. To obtain  $F_d$ , 10  $\mu\text{g}$  of trypsin is added into the cuvette. Separate experiments have verified that the fluorescences of the donor and acceptor GFPs are totally resistant to trypsin. This procedure causes complete dissociation of ECFP and EYFP.1 at room temperature within 10 min. As the fluorescence of EYFP.1 decreases, that of ECFP is dequenched to reach  $F_d$ . The obtained spectrum (Fig. 6, dotted line) is almost identical to that of ECFP only (Fig. 5), except for a tiny hump around 528 nm from EYFP.1 that is slightly cross-excited at 432 nm. Utilizing the  $F_d$ ,  $F'_{da}$ , and  $F''_{da}$  values, the FRET efficiencies of YC2.1 at saturating versus 14 nM free  $\text{Ca}^{2+}$  are calculated to be 54 and 25%, respectively.

## Quantifying Fluorescence Resonance Energy Transfer Efficiency

In the preceding discussion, the ratio of acceptor to donor emissions has been used as an index of the extent of FRET. This emission ratio is advantageous because it is the fluorescence parameter that is easiest to measure frequently and nondestructively while canceling out variations in cell thickness, excitation intensity, emission sensitivity, and overall indicator concentration. On the other hand, the observed emission ratio is still a function not only of the FRET efficiency but also the stoichiometry of acceptors relative to donors, the ratio of their quantum efficiencies, the relative efficiencies of the filters and detector(s) used to collect the emissions, the extent to which the excitation wavelength adventitiously excites the acceptor, and the extent to which the donor emission spills over into the acceptor emission band. Figure 5 shows that CFP can be selectively excited at 400–440 nm with little but not completely negligible direct excitation of YFP, but there is no wavelength at which YFP emission can be collected without including some direct emission from CFP. How do we disentangle the FRET efficiency or the extent of biochemical interaction from all these complicating factors? Several approaches have been employed in the literature, all of which have different advantages and restrictions.

### *Mathematical Correction*

In principle the perturbing parameters listed above could be carefully measured with pure samples of donor and acceptor, preferably using the same instrument as used for the actual biological measurement, if possible in cells similar to those in which the FRET is to be measured. With three fluorescence measurements (excitation of donor band, measurement at donor and acceptor emission bands; excitation of acceptor, measurement of acceptor emission), the stoichiometry of acceptors to donors can in principle be deduced and then corrected for, allowing extraction of the FRET efficiency.<sup>7</sup> In our view, the problems are that the mathematical formalism is complex and not intuitive, that the result often requires subtraction of nearly equal quantities and may therefore be sensitive to small errors in the correction parameters, and that the separate donor and acceptor samples must have the same optical properties (except for FRET) as the interacting partners.

### *Internal Calibration*

If the biological sample could be forced to two known states of high versus low protein association, faster than expression levels can change,

the emissions under those reference conditions can be used to calibrate previous or subsequent measurements on that sample. For example, if  $\text{Ca}^{2+}$  can be clamped *in situ* to high and low levels, using ionophores and chelators, emission ratios measured from the cells before  $\text{Ca}^{2+}$  clamping can be retrospectively calibrated in terms of the  $\text{Ca}^{2+}$  saturation of the indicator. Furthermore, if the titration curve for the indicator has been characterized *in vitro*, and it is assumed that it is the same in intact cells, the absolute  $[\text{Ca}^{2+}]$  concentrations may be calculated.<sup>13,14</sup> The problem is that for most novel protein interactions, it is not known how to turn the interaction on and off rapidly and completely *in situ*.

### External Calibration

In the external calibration approach, the emission ratio associated with the condition in which FRET is suspected (e.g., BFP-*X* and GFP-*Y*, where *X* and *Y* may form a heterodimer) is compared with that from separate cells in which FRET is unlikely to occur. Examples of such negative controls include transfections with unfused donor and acceptor GFP mutants (e.g., BFP and GFP), or fusions to noninteracting partners (e.g., BFP-*X* and GFP-*Z*, where *X* and *Z* do not interact), or fusions to the interacting partners but in the presence of a dominant-negative competitor such as excess unfused *X* or *Y*. A positive control such as BFP fused to GFP through an appropriate spacer may also be included for comparison.<sup>26</sup>

For example, to demonstrate a direct interaction between Bax and Bcl-2 proteins in mammalian cells, Mahajan *et al.*<sup>27</sup> coexpressed BFP-Bcl-2 and GFP-Bax fusion proteins in the same cells, and confirmed their colocalization within mitochondria. They then observed significant FRET from BFP to GFP when BFP-Bcl-2 was excited, fairly similar to that seen from a BFP-GFP fusion. In contrast, the green-to-blue emission ratio was much lower from a noninteracting pair of fusion proteins, cytochrome *c*-GFP and BFP-Bcl-2, coexpressed and observed in separate experiments. Similarly, Day<sup>26</sup> showed FRET between BFP fused to the transcription factor Pit-1 and the analogous GFP-Pit-1. Cotransfection of BFP-Pit-1 and GFP fused to a nuclear localization sequence was used as a negative control, while BFP fused to GFP through a three-amino acid linker was taken as a positive control.

The main problem with this general approach is that separate cells and transfections are being compared so that any variations in relative expression levels of the donor and acceptor constructs would produce artifactual variations in emission ratio, obscuring the effects of FRET. To go

<sup>26</sup> R. N. Day, *Mol. Endocrinol.* **12**, 1410 (1998).

<sup>27</sup> N. P. Mahajan, K. Linder, G. Berry, G. W. Gordon, R. Heim, and B. Herman, *Nature Biotechnol.* **16**, 547 (1998).



beyond a qualitative statement that FRET is occurring requires detailed mathematical corrections (see Mathematical Correction, above).

### *Donor Lifetime Measurement*

One of the most elegant methods for measuring FRET is to measure the excited state lifetime of the donor. For a homogeneous population, the energy transfer efficiency  $E$  is given not only by Eq. (1) but also by Eq. (2):

$$E = 1 - (\tau_{DA}/\tau_D) \quad (2)$$

where  $\tau_{DA}$  and  $\tau_D$  are the excited state lifetimes of the donor in the presence and absence of the acceptor, respectively.  $\tau_{DA}$  can be measured dynamically and nondestructively at every pixel of the image and compared with  $\tau_D$  measured from reference cells containing only donor. Only donor emission is monitored; emissions from the acceptor are disregarded, and large excesses of unbound acceptor have no effect. Because these lifetimes are independent of protein expression levels per se and most other perturbations, they should be quantitatively comparable from sample to sample. Several successful examples of FRET involving GFP mutants have been published.<sup>8,9,28</sup> The main disadvantage of lifetime imaging is that the equipment is expensive and not yet available in a ready-made commercial system. A subsidiary problem is that the usual and most accurate ways to determine lifetimes are wasteful of photons, for two reasons. Photons coming from the acceptor are discarded, even though they are the dominant emission if FRET is efficient, because the quantum yield of the acceptor GFP or YFP considerably exceeds that of the donor BFP or CFP. Also, the classic and most accurate means to measure lifetimes require that only emissions passing through narrow temporal or frequency windows are collected; these windows are systematically scanned to map the decay characteristics, but cause considerable photon losses requiring longer observation to compensate.

### *Acceptor Bleaching*

Equation (1) indicates that the efficiency of FRET is given by the extent of quenching of the donor when the acceptor is removed. For example, FRET from Cy3 to Cy5 has been quantified by photobleaching the Cy5.<sup>29</sup> The same principle is useful for quantifying the efficiency of FRET from

<sup>28</sup> T. Ng, A. Squire, G. Hansra, F. Bornancin, C. Prevostel, A. Hanby, *et al.*, *Science* **283**, 2085 (1999).

<sup>29</sup> P. I. Bastiaens, I. V. Majoul, P. J. Verveer, H. D. Soling, and T. M. Jovin, *EMBO J.* **15**, 4246 (1996).

CFP to YFP, because strong illumination at long wavelength ( $>500$  nm) bleaches YFP without affecting CFP, providing an optical means to eliminate YFP *in situ* whenever desired. Such bleaching is applicable to any CFP and YFP fusions inside cells under the microscope, whereas the trypsin cleavage described above (see Spectroscopic Analysis of YC2.1 Protein) is only feasible *in vitro* and depends on the linker being much more vulnerable to cleavage than the GFP mutants. No specialized equipment is required, unlike excited state lifetime imaging. Although the same principle might be tried with BFP and GFP, the differential bleaching with that pair would be more difficult because BFP is more photolabile than CFP, whereas GFP is more photostable than YFP. A unique feature of YFP, not shared by the other mutants or organic dyes, is that the bleaching is at least partly reversible by illumination at UV wavelengths.<sup>14,24</sup> Individual molecules of YFP can be seen to undergo many cycles of bleaching and regeneration, but in a large population of molecules the reversibility is not complete (see results below), so photobleaching is best done at the end of the experiment. It then provides a retrospective absolute calibration of FRET efficiency for the more sensitive and nondestructive dual-emission ratioing performed during cell dynamics. The following sections describe experiments using YFP photobleaching to quantify FRET in several systems.

### Split Yellow Cameleon-2.1

Split yellow cameleon-2.1 undergoes FRET between CFP and YFP, the efficiency of which is controllable by  $\text{Ca}^{2+}$ . It consists of an equimolar mixture of the two constituents of yellow cameleon-2.1: ECFP-CaM and M13-EYFP.1 (Fig. 7<sup>29a</sup>).<sup>13</sup> We first discuss how to measure the FRET efficiency when the components are saturated with  $\text{Ca}^{2+}$  to make a complex in a cuvette and in a solution under a microscope.

### Preparation of Purified Proteins

Recombinant proteins (ECFP-CaM and M13-EYFP.1) were expressed using the T7 expression system [pRSETB (InVitrogen)/JM109(DE3)]. *Escherichia coli* cells are transformed with the plasmids and selected at  $37^\circ$  on LB plates containing ampicillin ( $100 \mu\text{g/ml}$ ). A single colony is picked into 2 ml of LB medium containing ampicillin ( $100 \mu\text{g/ml}$ ), and grown overnight at  $37^\circ$ . A 100-fold dilution is made, and the culture is grown at room temperature until it reaches a density of approximately  $\text{OD}_{600}$  0.5, and then protein expression is induced with isopropyl- $\beta$ -D-thiogalactopyra-

<sup>29a</sup> M. Kozak, *J. Cell Biol.* **108**, 229 (1989).

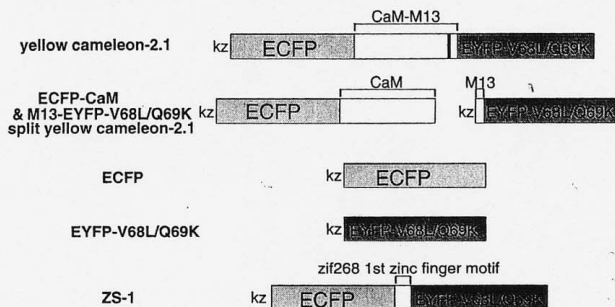


FIG. 7. Schematic structures of fusion proteins containing ECFP and/or EYFP.1 for mammalian expression. kz, Kozak sequence for optimal translational initiation in mammalian cells.<sup>29a</sup>

noside at a final concentration of 0.2 mM. Growth is continued for a further 12–24 hr. The cells are lysed with a French press, and the polyhistidine-tagged proteins are purified from the cleared lysates on nickel-chelate columns (Qiagen). The protein samples in the eluates are concentrated with a Centricon-30 (Amicon), and are further purified by gel-filtration or ion-exchange chromatography (Mono Q).

### *In Vitro Spectra of Split Yellow Cameleon-2.1*

Emission spectra of the purified proteins in a cuvette are measured with a fluorometer (SPEX Industries). ECFP–CaM and M13–EYFP.1 are mixed at 1:1 stoichiometry (5  $\mu$ M each) in a buffer [100 mM HEPES–KOH (pH 7.4), 50 mM KCl, 0.1 mM EGTA], and the two proteins dissociate completely (our unpublished results), resulting in no FRET (Fig. 8, left). The emission spectrum (excited at 432 nm) is almost identical to that of ECFP only, except for a small hump around 528 nm, which is from EYFP.1 cross-excited slightly at 432 nm. When  $\text{Ca}^{2+}$  is added to the solution at a final concentration of 1 mM, the 528 nm:476 nm emission ratio increases by about fourfold (Fig. 8, left). From Eq. (1) and the donor intensities at 476 nm with and without  $\text{Ca}^{2+}$ , an energy transfer efficiency in the  $\text{Ca}^{2+}$ -saturated state is calculated to be 0.43, assuming that the  $\text{Ca}^{2+}$ -free form has zero interaction and energy transfer efficiency.

### *Imaging Split Yellow Cameleon-2.1 in Solution under Microscope*

Bleaching of YFP is readily achieved under a microscope with a standard 150-W xenon lamp and a  $\times 40$  objective lens with high numerical aperture, such as 1.2 or greater. Proteins in solutions containing 50 mM HEPES–

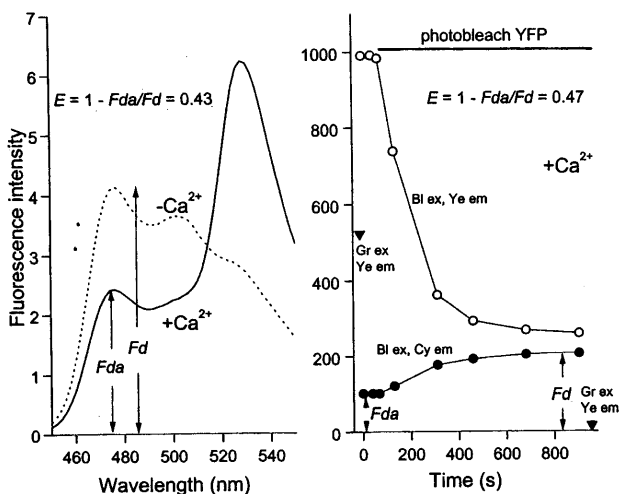


FIG. 8. FRET efficiency of split cameleon-2.1 saturated with  $\text{Ca}^{2+}$  *in vitro*. *Left*: Emission spectra of split yellow cameleon-2.1 in a cuvette, excited at 432 nm, at zero (dotted line) and saturating (solid line)  $\text{Ca}^{2+}$ . Fluorescence intensities at a wavelength of 476 nm are designated as  $F_d$  and  $F_{da}$ , respectively. *Right*: Fluorescence intensities through the FRET channel (535DF25, open circles labeled "Bl ex, Ye em"), donor channel (480DF30, closed circles labeled "Bl ex, Cy em"), and direct excitation of the acceptor (closed triangles labeled "Gr ex, Ye em") from a microscopic droplet containing split yellow cameleon-2.1 saturated with  $\text{Ca}^{2+}$  under light mineral oil. Intense illumination with a 540DF23 filter is indicated by the bar "photobleach YFP." The signals of the donor channel before and after the illumination are designated as  $F_{da}$  and  $F_d$ , respectively.

KOH (pH 7.4) and 50 mM KCl are injected through glass pipettes into light mineral oil on a coverslip. The droplets of the solutions are 50–150  $\mu\text{m}$  in diameter, so that they are completely confined within a field. Imaging is performed on a Zeiss Axiovert microscope with a cooled CCD camera (Photometrics, Tucson, AZ), controlled by MetaFluor 2.75 software (Universal Imaging, West Chester, PA).

First, ECFP-CaM and M13-EYFP.1 are separately injected into light mineral oil. They are imaged with blue and green excitations attenuated through neutral density filters of 1–4% transmission. Photobleaching is achieved by irradiating without neutral density filters through 535DF25 or 540DF23 interference filters from Omega Optical or Chroma Technologies (both Brattleboro, VT); the first number gives the center of the passband while the second number is the full width at half-maximal transmission, e.g., 540DF23 should pass 528.5–551.5 nm. These wavelengths are chosen to be on the long-wavelength edge of the YFP absorbance band in order

to minimize any chance of photobleaching CFP. After the completion of the work described below, we found that the above described passbands are unnecessarily conservative, in that a 525DF40 filter passing 505–545 nm bleaches YFP much faster but still avoids any damage to CFP (unpublished results of C. Y. Cho and R. Y. Tsien). YFP is regenerated with UV (330WB80: nominally 290–370 nm, but wavelengths below 330 nm are blocked by the glass objective). Although it is difficult to measure the power emerging from the objective in a microscopic beam of  $> 1.0$  NA, we did measure the power entering the objective as 16 and 3 mW for the 540DF23 and 330WB80 filters, respectively. Figure 9 (top) shows that EYFP.1, for example within M13–EYFP.1, can be completely bleached with  $\sim 540$  nm under conditions that have no effect on ECFP, for example within ECFP–CaM. The complete loss of long-wavelength EYFP.1 absorbance at this stage is also confirmed in another experiment, in which the protein in a cuvette is bleached by a laser at 532 nm, followed by measurement of absorbance. UV illumination causes partial recovery of the photobleached EYFP.1 ( $21 \pm 2\%$  of the original fluorescence intensity,  $n = 3$ ).

M13-YFP can be selectively photobleached without directly affecting CFP-CaM

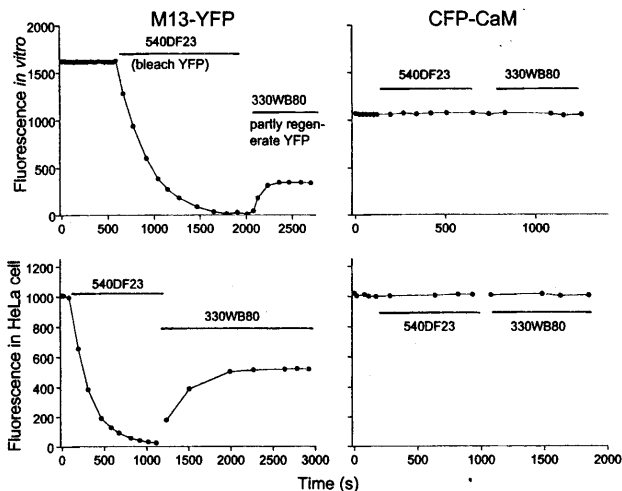


FIG. 9. Selective photobleaching of YFP *in vitro* (top) and in cells (bottom). M13–EYFP.1 in a droplet under mineral oil (top left) or expressed in HeLa cells (bottom left) was exposed to intense irradiation through 540DF23 and 330WB80 filters. The fluorescence intensity was monitored with a 495DF10 excitation filter, a 505DCLP dichroic mirror, and a 535DF25 emission filter. Likewise, ECFP–CaM under mineral oil (top right) and in HeLa cells (bottom right) was exposed to the same irradiation while monitoring its fluorescence with a 440DF20 excitation filter, a 455DRLP dichroic mirror, and a 480DF30 emission filter.

Figure 8 (right) shows a first test of the photobleach method to quantify FRET. A droplet of a 1:1 mixture of ECFP-CaM and M13-EYFP.1 in saturating<sup>2+</sup>, under mineral oil, is monitored by conventional emission ratioing using a 440DF20 excitation filter, a 455 DRLP dichroic mirror, and two emission filters (donor channel, 480DF30 for ECFP; FRET channel, 535DF25 for EYFP.1) alternated by a filter changer (Lambda 10-2; Sutter Instruments, San Rafael, CA). Photobleaching is performed as before; its completeness is verified by directly exciting the EYFP.1 via a 495DF10 excitation filter and a 505DCLP dichroic mirror, and monitoring through a 535DF25 emission filter. Bleaching reduces but does not eliminate the signal in the FRET channel; the residual emission is the cross-talk of the long-wavelength tail of ECFP into the yellow channel. Meanwhile the EYFP.1 bleaching dequenches the ECFP emission from  $F_{da}$  to  $F_d$ . The increase was 47% of  $F_d$ , corresponding to an energy transfer efficiency adequately close to that obtained in Fig. 8 (left) by comparing high versus low  $Ca^{2+}$ . But only the photobleach method is generalizable to live cells and to any pair of fusions to CFP and YFP.

### *Imaging Split Yellow Cameleon-2.1 within Cells under Microscope*

HeLa cells at 22° are imaged between 2 and 5 days after cDNA transfection with Lipofectin (GIBCO-BRL, Gaithersburg, MD). Selective bleaching of YFP is verified in HeLa cells separately expressing either ECFP-CaM or M13-EYFP.1 (Fig. 9, bottom). UV light restores a greater fraction ( $42 \pm 6\%$  of the original intensity,  $n = 8$ ) of EYFP.1 intensity in live cells than was possible *in vitro*. Perhaps the reducing environment of the cytoplasm partly inhibited irreversible photooxidative destruction of the EYFP.1.

A supramaximal dose (0.1 mM) of histamine in the presence of extracellular  $Ca^{2+}$  (1.3 mM) evokes a fairly long-lasting rise in cytosolic  $[Ca^{2+}]$  in HeLa cells, leading to as usual increase in the FRET channel and decrease in the donor ECFP channel (Fig. 10, top). During the stimulation, the EYFP.1 is deliberately photobleached and then partially regenerated, as shown by the images in Fig. 10 (bottom) obtained by direct excitation of the EYFP.1. The bleaching dequenches the ECFP to  $F_d$ , slightly above the donor emission before histamine ( $F_{da}$ ), indicating that there has been only 5.5% energy transfer efficiency in the unstimulated cells, consistent with a low but nonzero resting  $[Ca^{2+}]$ . The minimum ECFP emission at high  $[Ca^{2+}]$ ,  $F'_{da}$  corresponds to 42% energy transfer. Thus a single photobleach at the end of the experiment can retrospectively calibrate the energy transfer efficiency at all previous time points, assuming no bleaching or redistribution of the ECFP.

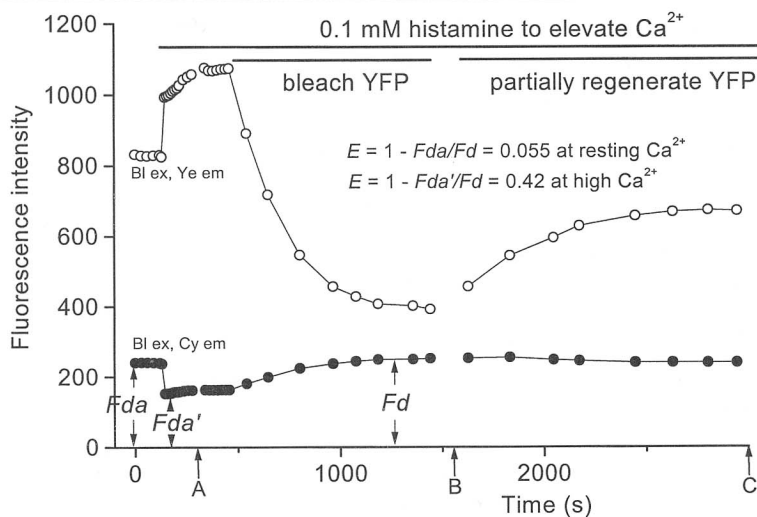


FIG. 10. Quantitation of FRET efficiency of split yellow cameleon-2.1 in a HeLa cell by the photobleaching method. *Top*: Emission intensities through the FRET channel (open circles) and donor channel (closed circles), both excited with a 440DF20 filter. The application of histamine and intense irradiation with 540DF23 and 330WB80 filters are indicated by horizontal bars. Fluorescence intensities of donor channel before ( $F_{da}$ ) and after ( $F'_{da}$ ) the addition of histamine, and after the 540DF23 illumination ( $F_d$ ) are shown by arrows. *Bottom*: Fluorescence images of the M13-EYFP.1 taken with a 495DF10 excitation filter, a 505DCLP dichroic mirror, and a 535DF25 emission filter at times A, B, and C indicated in the top graph. The pictures were printed with a fairly low-contrast printer that exaggerates the residual brightness at time B.

#### Photobleach Measurements of Fluorescence Resonance Energy Transfer in Yellow Cameleon-2.1 and between Unfused Cyan Fluorescent Protein and Yellow Fluorescent Protein

In yellow cameleon-2.1, the donor (ECFP) and the acceptor (EYFP.1) are joined by CaM and M13. Although the donor and acceptor can be

separated *in vitro* by trypsin (Fig. 6), trypsin cannot be applied within cells. However, photobleaching works in intact cells (Fig. 11) just as with the split cameleon. Application of 0.1 mM histamine followed by a 10  $\mu$ M concentration of an antagonist, cyproheptadine, produces a  $\text{Ca}^{2+}$  transient indicated by the reciprocal changes in the two emission intensities. After recovery of basal  $[\text{Ca}^{2+}]$ , the EYFP.1 is photobleached. The efficiency of FRET at the peak of  $\text{Ca}^{2+}$  transient (Fig. 11,  $F_{da}$ ) is 43%, similar to that for split yellow cameleon-2.1 (42%). The efficiency of FRET after recovery from histamine (Fig. 6,  $F'_{da}$ ) is 30%, indicating significant FRET even at basal  $\text{Ca}^{2+}$ , limited by the length of the CaM-M13 tether between the ECFP and EYFP.1 and any tendency for the two GFP mutants to dimerize. The 30 and 43% values for energy transfer efficiency are reasonably consistent with the trypsin-based measurements (Fig. 6) of 25 and 54% *in vitro*, considering that cytosolic  $\text{Ca}^{2+}$  does not traverse the full range from zero to saturating. Also in reasonable agreement, excited state lifetime imaging has yielded an independent measurement of 25% FRET for YC2 in unstimulated cowpea protoplasts.<sup>9</sup>

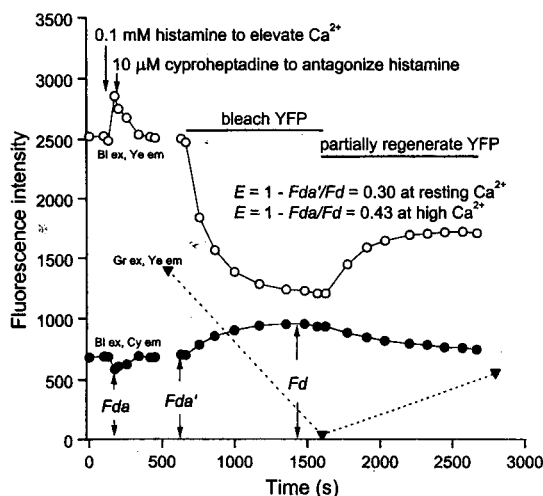


FIG. 11. FRET efficiency of intact yellow cameleon-2.1 in a HeLa cell measured by the photobleaching method as in Fig. 10. The fluorescence intensities of the donor channel during the  $\text{Ca}^{2+}$  transient ( $F_{da}$ ), after recovery from histamine ( $F'_{da}$ ), and after the 540DF23 illumination ( $F_d$ ) are shown by arrows. Fluorescence of directly excited EYFP.1 is indicated by filled triangles.



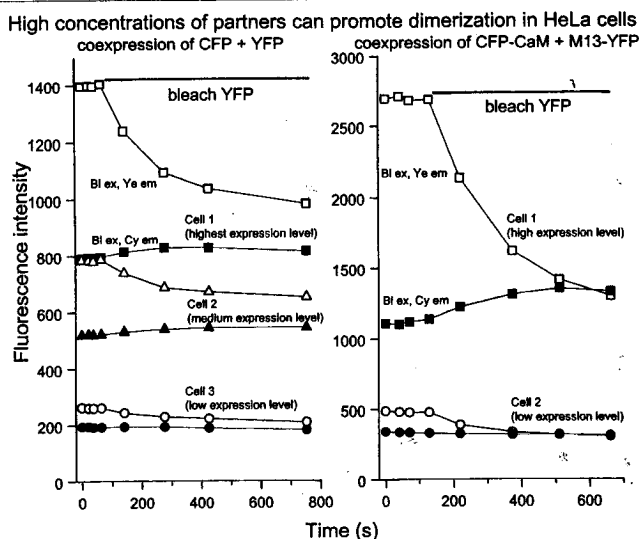


FIG. 12. Protein concentration-dependent FRET in unstimulated HeLa cells expressing ECFP and EYFP.1. *Left:* Fluorescence intensities through FRET and donor channels are shown by open and closed symbols, respectively, for three cells expressing estimated concentrations of  $300 \mu\text{M}$  (squares),  $200 \mu\text{M}$  (triangles), and  $80 \mu\text{M}$  (circles) of each of the two proteins. *Right:* Similar results for two cells coexpressing ECFP-CaM and EYFP.1 at high and low levels.

### Detection of Green Fluorescent Protein Dimerization inside Cells

Wild-type GFP undergoes changes in its absorption spectrum as a function of protein concentration,<sup>30</sup> implying some form of aggregation via hydrophilic and hydrophobic interactions, which are visible in some but not all GFP crystal forms.<sup>1,31</sup> Any intrinsic affinity of CFP and YFP for each other might also promote interactions between the fusion proteins containing the donor and acceptor GFPs, leading to artifactual interactions. To test whether ECFP and EYFP.1 interact at high concentrations *in vivo*, we expressed the two proteins in HeLa cells with identical promoters (Fig. 7) to achieve roughly equivalent expression levels. Concentrations of proteins in cells were estimated by knowing the thickness of cells and comparing their fluorescence brightness with those of known concentrations of fluorescent proteins in a wedge-shaped microchamber as previously described.<sup>14</sup> Figure 12 (left) shows data from three neighboring cells expressing different

<sup>30</sup> W. W. Ward, H. J. Prentice, A. F. Roth, C. W. Cody, and S. C. Reeves, *Photochem. Photobiol.* **35**, 803 (1982).

<sup>31</sup> F. Yang, L. G. Moss, and G. N. Phillips, Jr., *Nature Biotechnol.* **14**, 1246 (1996).

levels of each of the two proteins; the molar ratio of ECFP to EYFP.1 was almost one in each of the cells. When EYFP.1 was bleached, we observed slight but reproducible dequenching of ECFP fluorescence in cells containing high concentrations of proteins (cell *a*, squares, 300  $\mu\text{M}$ ; cell *b*, triangles, 200  $\mu\text{M}$ ), but not in cells with low concentrations (cell *c*, circles, 80  $\mu\text{M}$ ). Such concentration-dependent dimerization of GFP was also detected in unstimulated HeLa cells when split yellow cameleon-2.1 was highly concentrated (Fig. 12, right). It seems reasonable to assume that FRET in an CFP-YFP dimer, where the two proteins are touching one another, would be as strong as in  $\text{Ca}^{2+}$ -saturated cameleons or other covalent fusions incorporating CFP and YFP. Therefore the small FRET values obtained imply that dimerization is detectable but far from complete at the highest expression levels, as if the effective dissociation constant were in the millimolar range. A dissociation constant of 100  $\mu\text{M}$  for GFP homodimerization *in vitro* was estimated by analytical ultracentrifugation,<sup>32</sup> but large amounts of cytosolic proteins might well be somewhat competitive.

### Zinc Sensor Protein Analogous to Cameleons

Can the principle of the cameleons be adapted to measure analytes other than  $\text{Ca}^{2+}$ ? If the donor and acceptor are linked with just a CaM-binding peptide, then intermolecular binding of unlabeled  $(\text{Ca}^{2+})_4\text{-CaM}$  to the central peptide disrupts FRET.<sup>33</sup> This system has been used to determine free  $(\text{Ca}^{2+})_4\text{-CaM}$  concentrations in living cells.<sup>34</sup> To explore ions separate from  $\text{Ca}^{2+}$  signaling, we made a zinc sensor protein (ZS-1) by fusing ECFP and EYFP.1 with a linker of 39 amino acids corresponding to a zinc finger motif from a mouse transcription factor, *zif268* (Fig. 7). The cDNA for ZS-1 was created by replacing the *Sph1-Sac1* fragment for CaM-M13 in yellow cameleon-2.1 with a fragment encoding the first zinc finger motif of mouse *zif268* (from D. Saffen, University of Tokyo, Japan). The amino acid sequence of the introduced motif was MHERPYACPVESCDRRFRSRSDELTRHIRIHTGQKEL, in which amino acids conserved in this family of zinc fingers have been underlined. Figure 13 (left) shows the spectra of ZS-1 in a cuvette. FRET was considerable even in the absence of  $\text{Zn}^{2+}$ ; the emission ratio (535 : 480 nm) was 3.5, comparable to the ratio when the two GFP mutants were linked with floppy spacers.<sup>12</sup> In the presence of  $\text{Zn}^{2+}$  (0.1 mM), the ratio increased further to reach 6.7. The emission ratio change of the zinc sensor protein (ZS-1) was

<sup>32</sup> G. N. Phillips, *Curr. Opin. Struct. Biol.* **7**, 821 (1999).

<sup>33</sup> V. A. Romoser, P. M. Hinkle, and A. Persechini, *J. Biol. Chem.* **272**, 13270 (1997).

<sup>34</sup> A. Persechini and B. Cronk, *J. Biol. Chem.* **274**, 6827 (1999).

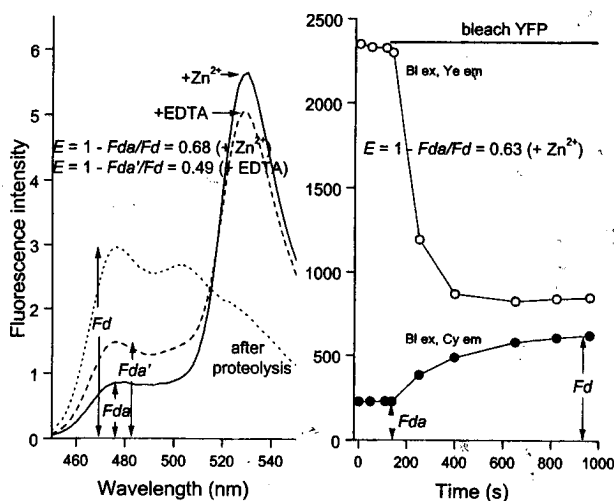


FIG. 13. Emission spectra and FRET efficiencies of a zinc sensor protein ZS-1 *in vitro*. *Left*: Emission spectra of ZS-1 in a cuvette, excited at 432 nm in 0.1 mM  $\text{ZnCl}_2$  (solid line), 0.3 mM EDTA (dashed line), and after proteolysis (dotted line). Fluorescence intensities at 476 nm when the protein was saturated with  $\text{Zn}^{2+}$  ( $F_{da}$ ) and proteolyzed ( $F_d$ ) are indicated. *Right*: Fluorescence intensities through FRET channel (open circles) and donor channel (closed circles) from a solution containing ZS-1 saturated with 0.2 mM  $\text{ZnCl}_2$  in mineral oil. The signals of the donor channel before and after photobleaching the acceptor are  $F_{da}$  and  $F_d$ , respectively.

$\text{Zn}^{2+}$  specific and reversible. After proteolysis by trypsin, the ratio went down to 0.65. Assuming no FRET after proteolysis, the efficiency of FRET was 49% in  $\text{Zn}^{2+}$ -free EDTA versus 68% when  $\text{Zn}^{2+}$  saturated. The latter value was checked by photobleaching the EYFP in a droplet under mineral oil on the microscope stage. The donor emission from ZS-1 with 0.1 mM  $\text{ZnCl}_2$  was quenched by 63% (Fig. 13, right), in adequate agreement with the estimate obtained by cleaving the linker. As far as we know, ZS-1 with  $\text{Zn}^{2+}$  has the highest efficiency of FRET for any CFP-YFP chimera so far. The transition dipoles of ECFP and EYFP.1 are presumably positioned to be even more favorable for FRET when the  $\text{Zn}^{2+}$  binding increases the ordering of the zinc finger motif.

## Conclusions

FRET between GFP mutants fused to host proteins has great potential as a general method for imaging dynamic changes in ligand concentrations

and the conformations and interactions of those host proteins.<sup>35</sup> Because a great deal of trial-and-error may be needed to optimize the spectral response, FRET readouts are not yet well suited to screening random libraries to find hitherto unknown partners. Instead, FRET can provide noninvasive monitoring with high spatial and temporal resolution of protein-protein interactions and ligand-induced conformational changes that are already known to be important and reasonably stoichiometric. Such measurements can be made much more quantitative by photobleaching the FRET acceptor, preferably a YFP, at the end of the experiment, because this easy step provides a reliable internal calibration of the FRET efficiency.

## Acknowledgments

This work was supported by the Howard Hughes Medical Institute, National Institutes of Health (NS27177 to R.Y.T.), and a Human Frontiers Science Program long-term fellowship to A.M.

<sup>35</sup> R. Y. Tsien and A. Miyawaki, *Science* **280**, 1954 (1998).